J Mol Model (2006) 12: 869–875
DOI 10.1007/s00894-006-0105-3

ORIGINAL PAPER

Qing Su · Lu Zhou

QSAR modeling of AT1 receptor antagonists using ANN

Received: 26 October 2005 / Accepted: 18 January 2006 / Published online: 16 March 2006

Abstract Multiple linear regression (MLR) and artificial neural networks (ANN) have been used for structure–activity relationship analysis for a set of 113 AT1 receptor antagonists. The ANN model showed better performance with a 6-6-1 architecture than MLR. The results obtained from this study indicate that three descriptors, hydration energy (EH), *n*-octanol/water partition (LOGP), and energy of the lowest unoccupied molecular orbital (LUMO), play an important role on the activity of AT1 receptor antagonists with biphenyltetrazole structures. This information is pertinent to the further design of new AT1 receptor antagonists.

Keywords Multiple linear regression · Artificial neural network · AT1 receptor antagonists · QSAR · Descriptors

Introduction

The rennin-angiotensin system (RAS) is an important element in the regulation of blood pressure and maintenance of electrolyte balance [1]. The RAS system elaborates several points for intervention and development of therapeutics for controlling hypertension. The angiotensin-converting enzyme (ACE) and rennin inhibitors have an established place in the management of hypertension [2, 3]. Because the active component in the RAS is angiotensin II (AII), antagonism of AII at the receptor (AT1) represents the most effective and specific way of RAS modulation. The discovery by the DuPont group of a series of (biphenylmethyl)imidazoles as nonpeptide, potent, and orally active AII receptor (AT1 subtype) antagonists has opened up a completely new field in AII antagonist research; the most representative structure in the series is Losartan (DuP-753, Fig. 1), which is already used for the treatment of hypertension in man.

The receptor site is a complex transmembrane unit for AII (AT1) that belongs to the superfamily of the seven transmembrane-domain receptors coupled with G-protein and the classic second messenger system. No doubt, it contains a variety of hydrophobic and hydrophilic regions. Previous studies [4] suggest that acid isosteres that are significantly ionized at physiological pH should have higher affinity for the receptor. The tetrazole moiety would be the most ionized of the three (tetrazole ring, –COOH, –SO_2NHCO–) commonly employed [5]. The biphenyltetrazole (BPT) (Fig. 1) compounds then were thought to possess better therapy effects and later AT1 receptor antagonists Valsartan and Candesartan, which including BPT moieties, soon confirmed this.

Quantitative structure-activity relationship (QSAR) models, mathematical equations relating chemical structure to their biological activity, give information that is useful for drug design and medicinal chemistry [6–8]. QSAR is largely used to predict activities and to define AT1 receptor antagonists [9, 10]. The objective of this investigation is to model experimentally determined IC_{50} values, which are the concentration of the antagonist that displaces 50% of specifically bound [125I][Sar1,Ile8]AII in a rabbit aorta from computationally derived molecular descriptors of BPT compounds, and to analyze the influence of descriptors, as well as to offer guidance for the design of this series of compounds.

Q. Su · L. Zhou (✉)
Department of Pharmaceutical Engineering,
College of Chemical Engineering,
Sichuan University,
Chengdu, Sichuan 610065, China
e-mail: zhouluscu@163.com
Tel.: +86-28-85403942
e-mail: sq7703@yahoo.com.cn

Materials and methods

Experimental data

Experimentally observed IC_{50} values for 113 BPT compounds were taken from the studies reported by Chang et al. [11] (Table 1), Winn et al. [12] (Tables 2, 3,

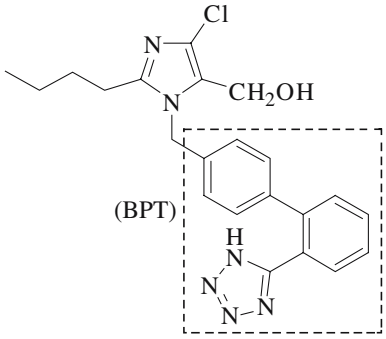

Fig. 1 Structure of Lorsartan

4), Mederski et al. [13] (Table 5), de Laszlo et al. [14] (Table 6), and Huang et al. [15] (Table 7). These data were collected in several different literature sources with experimental error of 20–25%. These values were converted to negative logarithm $\log(1/IC_{50})$ (briefly described as PIC50) as the dependent variable representing the biological activity of these compounds. The basic structures of these compounds are shown in Fig. 2 and the substituent patterns (SPs) of these compounds along with PIC50 used in this study are given in Tables 1, 2, 3, 4, 5, 6, 7.

Table 1 Substituent patterns (SPs) and PIC50 for basic structure (4)

Number	SPs	PIC50
1	H	7.66
2	2-Me	8.39
3	2-Cl	8.62
4	2-NO_2	9.07
5	2-OMe	8.18
6	3-Me	7.74
7	3-Cl	6.92
8	3-OMe	7.82
9	4-Cl	7.16
10	4-OMe	8.30
11	4-C_2H_5	7.57
12	4-F	7.68
13	4-COOMe	7.48
14	2-$CHMe_2$	8.85
15	2-C_6H_5	8.44
16	2-$CH_2C_6H_5$	7.96
17	2-F	8.11
18	2-Br	8.70
19	2-CF_3	8.92
20	2-COOMe	8.25
21	2-COOH	6.94
22	2-NH_2	7.00
23	2-NMe_2	8.50
24	2-NO_2,4-OMe	9.13

Molecular modeling and descriptor calculation

Molecular modeling calculations were performed using HyperChem 7.0 for Windows (Hypercube, FL, USA). The MM+ molecular mechanics force field was first run to approach to the optimized geometry. The conformation obtained from molecular mechanics was subjected to a refined geometry optimization using AM1 semiempirical molecular orbital theory. The AM1 Hamiltonian was selected because it gives good estimates of molecular energies and the computation time is much shorter than needed by ab initio methods. In this study, a set of descriptors related to physicochemical and geometrical properties of the molecules was used. All these descriptors are summarized in Table 8. Quantum chemical indices of hardness (η), softness (S), electronegativity (χ), chemical potential (μ), and electrophilicity (ω) were calculated according to the method proposed by Tanikaivelan et al. [16].

Multiple linear regressions (MLR)

This method was used to generate linear models between dependent variable and descriptors used with the software SPSS 12 running on a Pentium PC. Because of the many descriptors considered, a stepwise procedure combining the forward and backward algorithms was used to select the pertinent descriptors.

The molecules were divided into two sets: training and prediction sets. The training set was used to build linear models so that an accurate relationship could be found between structure and biological activity. The prediction set is a group of molecules not used to develop the model and serve as to test the predictive ability of the model with unknown compounds. These sets were created using the activity-binning method. This method consists of ranking the molecules according to their dependent-variable value and then populating the training and prediction sets such that the range of the dependent variable is represented within each set. This method resulted in the training set containing 103 molecules and the prediction set 10 molecules.

Artificial neural networks (ANN)

To test nonlinear effects on the data, the ANN technique was used in this study. In recent years, studies have demonstrated that ANN can be an effective tool for developing reliable QSAR [17–20]. The major advantage of ANN lies in the fact that QSAR can be developed without having to specify the analytical form of a particular correlation model. The neural-network approach is especially suitable for mapping complex nonlinear relationships that may exist between model output and model inputs.

The ANN program used was the neural-network software package of MATLAB 7.0.1 developed by Math Works. All neural networks were of the three-layer back-propagation type with batch-gradient descent with a

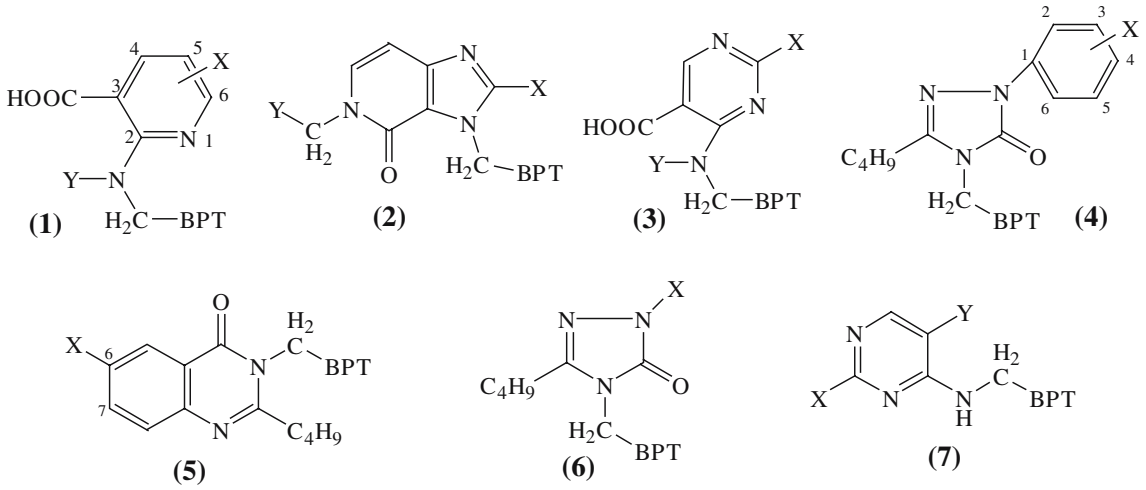

Fig. 2 Basic structures of compounds

variable learning-rate algorithm [21]. The tan-sigmoid transfer function was chosen for the neurons in the hidden layers. The linear transfer function was used in the output layer.

The molecules were divided into three sets: training, validation, and prediction. The training set was used to build the model and the prediction set was used to test the predictive ability of the model with unknown compounds. The validation set was used during the development of ANN models to prevent neural network overfitting. These sets were created using the activity-binning method described before. The method resulted in the training set containing 93 molecules, the validation set containing 10 molecules, and the prediction set containing 10 molecules.

Results and analysis

Multiple linear regression analysis

MLR analysis was performed on the compounds described in Tables 1, 2, 3, 4, 5, 6, 7, the PIC50 as the dependent variable, and the descriptors as the independent variables. A few suitable models were obtained and the results are shown in Table 9. Model 3 with the minimum root-mean-square (RMS) in Table 9 was regarded as the best linear model, and the coefficients of these models are shown in Table 10. The prediction set was used to test the predictive ability with model 3. The plots of calculated vs observed value of PIC50 from the best linear model are shown in Fig. 3.

To ensure that the results obtained in MLR were not due to chance and lend credence to our results, we ran a scrambling experiment. The dependent variable PIC50 was scrambled randomly, and then the same algorithms were used in MLR again. The statistical results as the RMS error

Table 2 Substituent patterns (SPs) and PIC50 for basic structure (1)

Number	SPs		PIC50
	X	Y	
25	H	C_3H_7	10.10
26	4-Me	C_3H_7	9.64
27	5-Me	C_3H_7	8.80
28	5-Cl	C_3H_7	9.07
29	5-F	C_3H_7	9.04
30	5-I	C_4H_9	8.38
31	5-C_5H_6	C_3H_7	8.91
32	5-NH_2	C_3H_7	7.60
33	5-NHCOMe	C_3H_7	7.90
34	6-Me	C_4H_9	8.15
35	6-F	C_3H_7	9.63
36	6-OMe	C_3H_7	7.78

Table 3 Substituent patterns (SPs) and PIC50 for basic structure (3)

Number	SPs		PIC50
	X	Y	
37	H	H	5.61
38	Me	H	7.50
39	C_2H_5	H	8.30
40	C_3H_7	H	8.27
41	C_4H_9	H	7.91
42	C_5H_{11}	H	7.23
43	CH_2CH_2OMe	H	6.81
44	C_4H_9	Me	7.15
45	Me	C_2H_5	7.96
46	Me	C_3H_7	9.60
47	Me	C_4H_9	8.81
48	Me	C_5H_{11}	8.73
49	Me	$CH_2CH{=}CH_2$	8.32
50	Me	CH_2CHMe_2	7.50
52	Me	CH_2CH_2OMe	8.50
52	H	C_3H_7	9.68
53	H	C_4H_9	9.57
54	C_3H_7	C_3H_7	8.52
55	SMe	C_4H_9	8.38

Table 4 Substituent patterns (SPs) and PIC50 for basic structure (7)

Number	SPs		PIC50
	X	Y	
56	H	$CO_2C_2H_5$	6.24
57	Me	$CO_2C_2H_5$	7.13
58	C_2H_5	$CO_2C_2H_5$	7.78
59	C_3H_7	$CO_2C_2H_5$	7.91
60	C_4H_9	$CO_2C_2H_5$	7.37
61	C_5H_{11}	$CO_2C_2H_5$	6.37
62	CH_2CH_2OMe	$CO_2C_2H_5$	7.10
63	Me	CH_2OH	7.12
64	C_2H_5	CH_2OH	7.96
65	C_3H_7	CH_2OH	7.60
66	C_4H_9	CH_2OH	7.53
67	CH_2CH_2OMe	CH_2OH	6.41

Table 5 Substituent patterns (SPs) and PIC50 for basic structure (2)

Number	SPs		PIC50
	X	Y	
68	C_4H_9	COC_6H_5	8.40
69	C_4H_9	$COCMe_3$	9.40
70	C_4H_9	COOMe	9.70
71	C_4H_9	COOH	9.16
72	C_4H_9	$CONH_2$	9.40
73	C_4H_9	$CONMe_2$	9.70
74	C_3H_7	$CONMe_2$	10.00
75	C_2H_5	$CONMe_2$	9.52
76	C_4H_9	$CON(C_2H_5)_2$	10.10
77	C_2H_5	$CON(C_2H_5)_2$	9.52
78	C_4H_9	CO-pyrrolidino	9.70
79	C_2H_5	CO-piperidino	9.70
80	C_4H_9	$CONHC_6H_5$	9.00
81	C_4H_9	$CON(Me)C_6H_5$	9.52

Table 6 Substituent patterns (SPs) and PIC50 for basic structure (5)

Number	SPs	PIC50
82	H	8.22
83	Me	8.40
84	$CHMe_2$	8.30
85	C_2H_5	8.40
86	SMe	8.16
87	SOMe	9.00
88	F	7.59
89	Cl	7.54
90	OH	7.57
91	$OCONHCHMe_2$	9.00
92	OMe	8.30
93	OMe, 7-OMe	7.89
94	NH_2	8.89
95	NHCOMe	8.05
96	$NHCO(CH_2)_3CH_3$	8.70

Table 7 Substituent patterns (SPs) and PIC50 for basic structure (6)

Number	X	PIC50
97	H	7.38
98	C_2H_5	7.66
99	$(CH_2)_2CH_3$	7.82
100	$(CH_2)_3CH_3$	8.29
1010	$(CH_2)_4CH_3$	8.25
102	$(CH_2)_5CH_3$	8.06
103	$(CH_2)_7CH3$	6.77
104	$CHMe_2$	7.70
105	$CHMeCH_2CH_3$	8.00
106	$CH_2CHMeCH_2CMe_3$	7.46
107	$CH_2COOCH_2CH_3$	8.05
108	$CH_2CO_2CMe_3$	7.80
109	$(CH_2)_4COOCH_3$	8.36
110	$(CH_2)_5COOCH_2CH_3$	8.01
111	C_6H_5	7.23
112	$CH_2CH_2C_6H_5$	8.51
113	$(CH_2)_3C_6H_5$	7.75

Table 8 The calculated descriptors used in this study

Descriptor	Brief Description
ET	Total molecular energy
EB	Molecular binding energy
EI	Molecular isolated atomic energy
EE	Molecular electronic energy
EC	Molecular core–core interaction energy
HF	Heat of molecular formation
DM	Total molecular dipole moment
SM	Molecular surface area
VM	Molecular volume
EH	Hydration energy
LOGP	*n*-octanol/water partition
RM	Molecular molar refractivity
PM	Polarizability of molecule
MM	Mass of molecule
HOMO	Energy of the highest occupied molecular orbital
LUMO	Energy of the lowest unoccupied molecular orbital
χ	Electronegativity; −0.5(HOMO−LUMO)
η	Hardness; 0.5(HOMO+LUMO)
S	Softness; $1/\eta$
ω	Electrophilicity; $\chi^2/2\eta$

Table 9 Model summary of multiple linear regression analysis

Model	RMS	Descriptors
1	0.6673	EH, LOGP, RM, PM, LUMO, S, ω
2	0.6671	EH, LOGP, RM, PM, LUMO, ω
3	0.6639	EH, LOGP, RM, PM, LUMO
4	0.6669	EH, LOGP, RM, PM
5	0.6714	EH, RM, PM

Table 10 The coefficients of linear model

Descriptors	(Constant)	ω	EH	HF	LUMO	LogP	RM	PM	S
Coefficients of model 1	−78.42	−17.22	0.005	0.002	−17.07	0.125	0.515	−1.302	−196.85
Coefficients of model 2	1.693	−0.415	0.005	N/A	−1.487	0.125	0.519	−1.315	N/A
Coefficients of model 3	2.766	N/A	0.005	N/A	−1.363	0.127	0.514	−1.308	N/A
Coefficients of model 4	3.850	N/A	0.005	N/A	N/A	0.09	0.521	−1.318	N/A
Coefficients of model 5	3.951	N/A	0.004	N/A	N/A	N/A	0.433	−1.075	N/A

of its results were compared with that of the MLR models developed in this work. The RMS ranged from 0.005 to 0.4. This appears to indicate that chance correlation did not play a significant role in the results described above.

Artificial neural network (ANN)

The neural-network approach is especially suitable for analyzing complex nonlinear relationships between the outputs and inputs. The network inputs and outputs were preprocessed to make the training more efficient. Initially, inputs and outputs were normalized so that they fall in the range of [−1, 1]. After the network has been trained, the outputs need to be transferred back to the same units that were used for the original outputs for comparison purpose.

Input data of the model with highly correlated or redundant information would greatly increase the complexity of model and would be bad for the accuracy of model, so the descriptors used for training should be selected before training. This was carried out in two steps. Firstly, the correlation coefficients were calculated for all descriptors in the pool (see Table 11). According to the correlation-coefficient matrix, descriptors were partitioned into several groups with descriptors in one group having a correlation coefficient greater than a user-specified cutoff (0.8 in this case). Secondly, sensitivity analysis of descriptors was used to select descriptors from each group. The correlation coefficients between descriptors and dependent variable were determined (see Table 12). The higher the correlation coefficient of descriptor, the greater its influence on the model. Hence, those descriptors with the highest correlation coefficient for each group were selected. Finally, six descriptors, molecular electronic energy (EE), hydration energy (EH), *n*-octanol/water partition (LOGP), total molecular dipole moment (DM), electrophilicity (ω), and lowest unoccupied molecular orbital (LUMO), were selected to build the nonlinear model.

The number of neurons in the hidden layer is an important factor determining the network's performance. That is, too many nodes cause the network to memorize the dateset (overfitting); networks with few nodes may be insufficient to use all the information from the dataset (underfitting). It is desirable to construct the network that generalizes the patterns of the dataset rather than that merely memorizes them [22]. Previous studies conducted to determine the appropriate number of hidden units suggest that ρ, the ratio of the number of data points to the

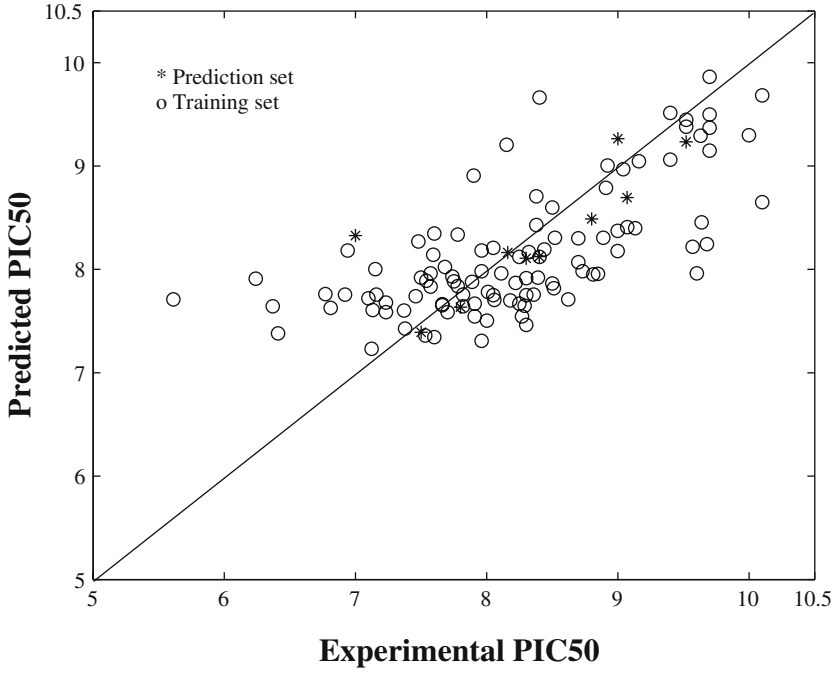

Fig. 3 A plot of observed vs predicted PIC50 values from the best linear model

Table 11 Correlation matrix (r value) of descriptors for each molecule

	ET	EB	EI	EE	EC	HF	DM	SM	VM	EH	LOGP	RM	PM	MM	HOMO	LUMO	χ	η	S
EB	0.87	1																	
EI	0.99	0.86	1																
EE	0.95	0.94	0.95	1															
EC	−0.95	−0.94	−0.94	−0.99	1														
HF	−0.12	−0.31	−0.11	−0.19	0.19	1													
DM	0.07	−0.05	0.08	0.1	−0.1	0.15	1												
SM	−0.47	−0.49	−0.46	−0.43	0.43	0.18	0.17	1											
VM	−0.84	−0.96	−0.83	−0.86	0.85	0.36	0.16	0.56	1										
EH	−0.69	−0.65	−0.69	−0.71	0.7	−0.06	−0.03	0.34	0.6	1									
LOGP	−0.09	−0.3	−0.08	−0.12	0.12	0.35	0.62	0.24	0.41	−0.1	1								
RM	−0.88	−0.96	−0.87	−0.94	0.94	0.37	0.02	0.47	0.93	0.64	0.27	1							
PM	−0.87	−0.96	−0.86	−0.93	0.93	0.38	0.06	0.48	0.94	0.63	0.33	0.99	1						
MM	−0.92	−0.89	−0.92	−0.92	0.92	0.27	−0.01	0.48	0.89	0.65	0.23	0.96	0.95	1					
HOMO	−0.41	−0.54	−0.39	−0.43	0.43	0.44	0.18	0.39	0.55	0.23	0.17	0.57	0.56	0.47	1				
LUMO	0.28	0.01	0.29	0.23	−0.22	0.1	0.45	0.06	0.05	−0.2	0.54	−0.1	−0.06	−0.19	0.12	1			
χ	0.47	0.55	0.46	0.49	0.49	−0.42	−0.07	−0.37	−0.53	−0.28	−0.04	−0.59	−0.58	−0.51	−0.97	0.12	1		
η	−0.32	−0.51	−0.31	−0.36	0.36	0.44	0.27	0.38	0.53	0.17	0.29	0.52	0.52	0.40	0.97	0.34	−0.89	1	
S	0.31	0.50	0.3	0.35	−0.35	−0.43	−0.27	−0.37	−0.52	−0.16	−0.28	−0.51	−0.51	−0.39	−0.97	−0.36	0.89	−0.99	1
ω	−0.52	−0.5	−0.51	−0.52	0.51	0.35	−0.07	0.32	0.47	0.31	−0.12	0.57	0.54	0.53	0.85	−0.41	−0.95	0.72	−0.72

Table 12 Correlation coefficients between descriptors and dependent variable

Descriptor	ET	EB	EI	EE	EC	HF	DM	SM	VM	EH	LOGP	RM	PM	MM	HOMO	LUMO	χ	η	S	ω
PIC50	−0.41	−0.34	−0.41	−0.43	0.42	0.05	−0.27	0.18	0.26	0.40	−0.23	0.40	0.35	0.39	0.19	−0.33	−0.27	0.11	−0.11	0.35

number of adjustable weights in the neural network, should have a value between 1.8 and 2.3 [22, 23]. The range of ρ was used as a guideline for an acceptable number of neurons in the hidden layer. When the increase of hidden neurons did not improve the model anymore, where the performance of the neural network model was evaluated with the combination of the RMS errors of the training and validation set, several of the suitable nonlinear models are summarized in Table 13. The architecture of 6-6-1 with minimum RMS of training and prediction set was selected as the best nonlinear model. The prediction set was used to test the predictive ability with architecture 6-6-1. The plots of calculated vs observed values of PIC50 from the best nonlinear model are shown in Fig. 4.

To ensure that the results obtained in the ANN were not due to chance and lend credence to our results, the scrambling experiment described before was used and the RMS ranged from 0.002 to 0.3. This appears to indicate that chance correlation did not play a significant role in the results described above.

The RMS for the training sets of the linear model were all greater than 0.6, and the RMS for the training and validation sets of the nonlinear model were all lower than 0.6, which indicated that the nonlinear model was better than the linear model during the training process. For the prediction ability, the RMS of best linear and nonlinear models were 0.4852 and 0.2245, respectively, which indicated that the predictive ability of best nonlinear model was better than that of best linear model. As can be seen from Fig. 3 and Fig. 4, the points of Fig. 3 are scattered while the points of Fig. 4 were spread along with the line closely, which also indicated that the nonlinear model showed better performance than the linear model. The reasons that the linear model performed poorly were likely because of the diversity of compounds and the widely varying experimental conditions.

The final descriptors used in the best linear model were EH, LOGP, RM, PM, and LUMO while those in the best nonlinear model were EE, EH, LOGP, DM, ω, and LUMO. Three descriptors EH, LOGP, LUMO all used in MLR and ANN indicated that they played a more important role on the biological activity of these compounds. To ensure that the subset of descriptors used in the best linear and nonlinear models were specific for their model, the subsets of descriptors used in the best nonlinear and linear models were exchanged to build linear and nonlinear models. In all

Table 13 The influence of different hidden neurons on the ANNs' performance

ANNs[a]	RMStr	RMSval
6-4-1	0.5887	0.5965
6-5-1	0.5459	0.4662
6-6-1	0.136	0.3909
6-7-1	0.4518	0.441
6-8-1	0.5802	0.5922

[a]Number of inputs-hidden-outputs neurons

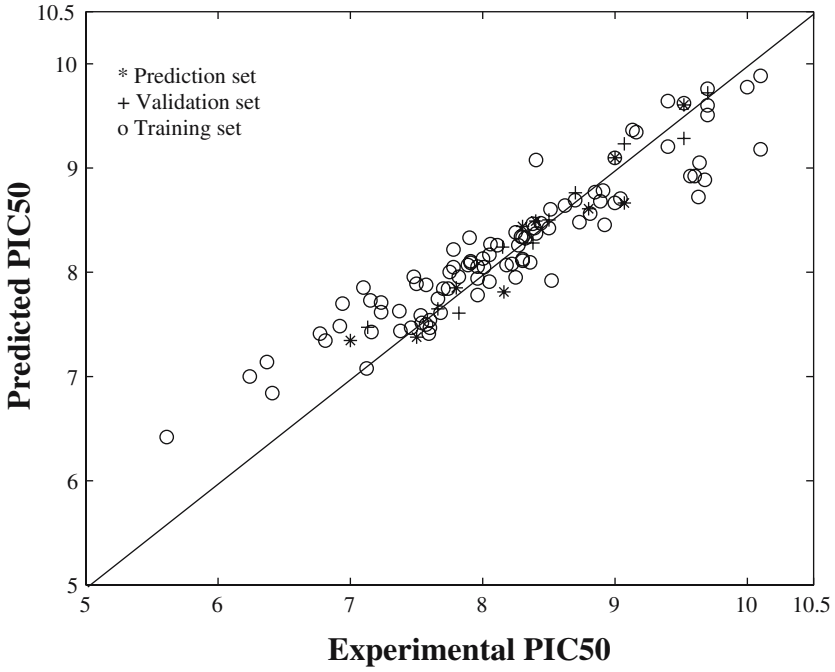

Fig. 4 A plot of observed vs predicted PIC50 produced from the best nonlinear model using a 6-6-1 architecture

cases, the resultant models performed poorly in comparison to the best models reported in this work.

Conclusions

MLR and ANN have been used for the model and prediction of PIC50 value from computationally derived molecular descriptors of BPT compounds; the pattern obtained with the ANN approach was more efficient than MLR analysis.

In this study, the complex nature of modeled biological activity of the AT1 receptor antagonist was taken into account. Our results indicated that three descriptors, EH, LOGP, LUMO, were important for the biological activity of BPT analogues with diversity structures. The result revealed good stability of structure–activity relationship studied, and confirmed the fact that biological activity depends, in a great part, on the structural features of the compounds.

Acknowledgement This work was partially supported by China West Medical College.

References

1. Vallotton MB (1987) Trends Pharmacol Sci 8:69–74
2. McAreavey DW, Robertson JIS (1990) Drugs 40:326–345
3. Greenlee WJ (1990) Med Res Rev 10:173–236
4. Noda K, Saad Y, Kinoshita A, Boyle TP, Graham RM, Husain A, Karnik SS (1995) J Biol Chem 270:2284–2289
5. Kurup A, Garg R, Carini DJ, Hansch C (2001) Chem Rev 101:2727–2750
6. Hadjipavlou-Litina D (1998) Med Res Rev 18:91–119
7. Gramatica P, Papa E (2003) QSAR Comb Sci 22:374–385
8. Hansch C, Kurup A, Garg R, Gao H (2001) Chem Rev 101:619–672
9. Datar P, Desai P, Coutinho E, Iyer K (2002) J Mol Model 8:290–301
10. Datar PA, Desai PV, Coutinho EC (2004) J Chem Inf Comput Sci 44:210–220
11. Chang LL, Ashton WT, Flanagan KL, Strelitz RA, Maccoss M, Greenlee WJ, Chang RSL, Lotti VJ, Faust KA, Chen TB, Bunting P, Zingaro GJ, Kivlighn SD, Siegl PKS (1993) J Med Chem 36:2558–2568
12. Winn M, De B, Zydowsky TM, Altenbach RJ, Basha FZ, Boyd SA, Brune ME, Buckner SA, Crowell D, Drizin I, Hancock AA, Jae HS, Kester JA, Lee JY, Mantei RA, Marsh KC, Novosad EI, Oheim KW, Rosenberg SH, Shiosaki K, Sorensen BK, Spina K, Sullivan GM, Tasker AS, von Geldern TW, Warner RB, Opgenorth TJ, Kerkman DJ, Debernardis JF (1993) J Med Chem 36:2676–2688
13. Mederski WWKR, Dorsch D, Bokel HH, Beier N, Lues I, Schelling P (1994) J Med Chem 37:1632–1645
14. de Laszlo SE, Allen EE, Quagliato CS, Greenlee WJ, Patchett AA, Nachbar RB, Sieg KS, Chang RS, Kivlighn SD, Schorn TS, Faust KA, Chen TB, Zingaro GJ, Lotti VJ (1993) Bioorg Med Chem Lett 3:1299–1304
15. Huang HC, Reitz DB, Chamberlain TS, Olins GM, Corpus VM, McMahon EG, Palomo MA, Koepke JP, Smits GJ, McGraw DE, Blaine EH, Manning RE (1993) J Med Chem 36:2172–2181
16. Thanikaivelan P, Subramanian V, Rao JR, Nair BU (2003) Chem Phys Lett 323:59–70
17. Schaper KJ, Samitier MLR (1997) Quant Struct-Act Relatsh 16:224–230
18. Huuskonen JJ, Livingstone DJ, Tetko IV (2000) J Chem Inf Comput Sci 40:947–955
19. Breindl A, Beck N, Clark T, Glen RC (1997) J Mol Model 3:142–155
20. McClelland HE, Jurs PC (2000) J Chem Inf Comput Sci 40:967–975
21. Hagan MT, Demuth HB, Beale MH (1996) Neural network design, 1st edn. PWS, USA, pp 45–67
22. Andrea TA, Kalayeh H (1991) J Med Chem 34:2824–2836
23. So SS, Richards WG (1992) J Med Chem 35:3201–3207